Chapter 10
Time Series Analysis of Satellite Remote Sensing Data for Monitoring Vegetation and Landscape Dynamics of the Dried Sea Bottom Adjacent to the Lower Amu Darya Delta

Rainer A. Ressl and René R. Colditz

Abstract The Aral Sea region is a rapidly transforming landscape due to the continuous desiccation process. This study describes the vegetation and landscape dynamics in the lower Amu Darya Delta and adjacent parts of the dried sea bottom using MODIS (Moderate Resolution Imaging Spectroradiometer) surface reflectance data and EVI time series for the years 2001–2011. The potential of MODIS time series for monitoring landscape and vegetation dynamics of the dried sea bottom adjacent to the lower Amu Darya Delta was evaluated concerning data availability and spatial and temporal resolution. Two time series with different quality considerations were generated to subsequently characterize the yearly changes in the dried part of the sea bed, a simple layerstack (LS) of observations and quality-filtered and smoothed time series using a double logistic function (DL). The EVI (Enhanced Vegetation Index) values show a small dynamic inter- and intra-annual range. The majority of the EVI values fluctuate between −0.2 and +0.1, which indicates generally low vegetation dynamics in the desiccated areas. Looking at the inter-annual behavior of the LS/DL time series plots, the noise of the data and data fluctuations seem to become less for areas which have been dry for a longer period. A regional differentiation of the landscape dynamics between the Eastern and the Western basin of the southern Aral Sea could be observed. The observation points for the Western basin show a more stable behavior of the EVI values in comparison to the samples on the Eastern basin as seasonal or inter-annual flooding is less frequent. A typical pattern as a result of clear vegetation dynamics could not be observed in the EVI, LS and DL time series plots.

Keywords Aral Sea • Time series • EVI • MODIS • Desiccation • Landscape dynamics

R.A. Ressl (✉) • R.R. Colditz
The National Commission for the Knowledge and Use of Biodiversity (CONABIO), Liga-Periferico Insurgentes Sur 4903, Col. Parques de Pedregal, Del. Tlalpan, C.P 14010, Mexico D.F, Mexico
e-mail: Rainer.Ressl@conabio.gob.mx

P. Micklin et al. (eds.), *The Aral Sea*, Springer Earth System Sciences,
DOI 10.1007/978-3-642-02356-9_10, © Springer-Verlag Berlin Heidelberg 2014

10.1 Introduction

Remote sensing time series have been widely used for land cover and land use monitoring at different regional scales. The Advanced Very High Resolution Radiometer (AVHRR) on board the TIROS-N and NOAA satellites has provided coarse spatial resolution data since 1981 at different levels of processing (Kidwell 1991; Tucker et al. 2005). Since the end of the millennium additional monitoring alternatives are available using data of the Sea-viewing Wide Field-of-view Sensor (SeaWiFS), the Système Pour l'Observation de la Terre – Vegetacion (SPOT VGT), Environmental Satellite's (ENVISAT) Advanced Along Track Scanning Radiometer (AATSR) and Medium Resolution Imaging Spectrometer (MERIS) instruments as well as the Moderate resolution Imaging Spectroradiometer (MODIS) on board the Terra (EOS-AM1) and Aqua (EOS- PM1). All systems have a spatial resolution of 1 km except for MERIS with 300 m and MODIS with bands of 250 and 500 m spatial resolution but more and better-calibrated bands than AVHRR. The high temporal resolutions of these imaging sensors have shown to be useful for describing the temporal dynamics of seasonal changes in vegetation and land use (Hansen et al. 2000; Ginzburg et al. 2010).

Thenkabail et al. (2005) showed the usefulness of temporally continuous MODIS data for land cover and land use classification in different river basins. Ressl et al. (1996, 1998) have demonstrated the applicability of multi-temporal AVHRR data to monitor and quantify the desiccation process of the Aral Sea and subsequently the use of these data for crop phenology monitoring and crop water consumption estimation. However, studies using this sensor were limited because of the coarse spatial resolution, 1.1 km for local area coverage and 4 km for global area coverage, and spectral resolution with only five bands. With the launch of the Aqua and Terra-MODIS satellites essential improvements have been made concerning the spatial and spectral resolution, the availability of the data and of derived products in comparison with the NOAA-AVHRR satellite generations. The instruments acquire each day since 2000 (Terra) and 2002 (Aqua) multiple images over the study area and therefore provide a favorable data source for multi-temporal studies and time series analysis. Their improved spatial resolution up to 250 m and 36 spectral bands allow for better product calibration and provide unique opportunities for regional to global studies. The MODIS data processing system operationally corrects for radiometric, geometric, and atmospheric issues and offers a large suite of value-added and modeled products (Justice et al. 2002). In addition, the facilitated access to data and to standardized products such as the Normalized Difference Vegetation Index (NDVI), the Enhanced Vegetation Index (EVI), Land Surface Temperature (LST) and Leaf Area Index (LAI), etc. enabled an enhanced monitoring of the desiccation process of the Aral Sea and associated changes and landscape dynamics in the surrounding newly-formed dry lands (Micklin 2004, 2007).

Landsat TM data with 30 m spatial resolution and seven bands may seem to be an interesting alternative but the small satellite swath width of only 180 km requires

mosaicing of multiple passes and may result in only 2–3 cloud-free coverages per year. Newer satellite constellations providing multiple satellites in orbit, such as the Rapideye system (5 satellites) or the DMC multi-nation satellite constellation combine high spatial resolution with a much more enhanced temporal resolution. These constellations provide excellent optical data to monitor dynamic processes, but are commercial systems.

Detailed studies concerning vegetation and landscape dynamics as well as the botanical diversity of the deltaic plains in the lower Amu Darya River Delta were carried out by Ptichnikov (2002) and Novikova (1996a, 1997) on the basis of intensive field work but also using Landsat TM data to provide a synergistic view of the ecological situation.

More recent studies in the Amu Darya Delta include the landscape dynamics, ecosystem and crop monitoring studies of Loew et al. (2012) and Conrad et al. (2007). The former applied multi-temporal MODIS time series of the years 2000, 2004 and 2008 to monitor landscape dynamics for these time intervals and the latter to derive land cover and land use information and to quantify spatio-temporal water use patterns.

The main goal of this study is to investigate the usefulness of non-commercial satellite data time series to monitor general landscape dynamics of the recently dried seabed of the Aral Sea and adjacent areas in the lower Amu Darya Delta. In particular the worth of MODIS time series is evaluated and related to the following issues:

- Qualitative analysis of the inter-annual development of the annually dried seabed
- Qualitative analysis of the intra-annual landscape dynamics using MODIS EVI products
- Plant succession dynamics monitoring on newly dried seabed with respect to different time series length (years)
- Analysis of data availability of MODIS time series with respect to data quality

10.2 Study Area

The southern Aral Sea region was selected as the study area to evaluate the usefulness of MODIS satellite time series to monitor landscape dynamics and plant succession states. The desiccation process of the Aral Sea is most prominent in the lower Amu Darya Delta region adjacent to the southern extensions of the remaining water bodies of the large Aral Sea, which can be divided into the Western and Eastern basin. Every year large extents of the former water body are exposed as newly dry seabed. Numerous studies have documented this dynamic process through satellite data (Ressl 1996; Micklin 2007) but few studies have investigated the rate of plant succession and the general landscape dynamics on these very recent dried-up seabed areas. Studies on areas, that have fallen dry since the early 1960s

when the desiccation process started, are manifold. Novikova (1996b) provides an extensive overview on landscape dynamics within these desiccated zones and on plant succession states and their associated ecology in the lower Amu Darya Delta.

The landscape of the dry seabed is very diverse and usually presents a complex mixture of sandy and saline soils. Plants actively colonize these slowly developing ecosystems, where the basis for the plant colonization primarily consists of flora of the Aral Sea terraces and the surrounding mainland of the Aral Sea. These highly salt-tolerant halophytes show different strategies towards the regulation of the high salt content of the solonchak soils.

The continuous process of the succession of the pioneer plants is an important factor for the stabilization of soils. Due to the vast newly dried seabed of the southern Aral Sea, every year large areas are exposed to the frequent strong winds and storms in the region. Thus, this salt desert, occasionally also referred to as the "Aralkum", has become the main source for salt and dust storms in the last decades threatening the health of the population living in the Amu Darya Delta. The yearly estimates of the salt and dust load range from 40 to 150 million tons per year, resulting in a major highly negative impact on the fertility of important agricultural production sites (Glazovskiy 1990).

Reducing the desertification process and stabilizing the surface against wind erosion is not an easy task. The natural process of plant colonization through halophytes and xerophytes is slow and can last decades before becoming effective. Phytomelioration has been increasingly discussed as a means to fight and reduce desertification in the region. Widespread plantations of adapted desert vegetation, such as the white and black saxaul (Haloxylon aphyllum) are appraised as favorable to stabilize the desiccated seafloor. Studies on the natural process of plant succession on the former seabed show that in the first years after drying, exogenic factors such as geomorphological and edaphic processes are dominating the ecosystem and landscape dynamics (Breckle et al. 2012).

10.3 Data and Preprocessing

In this study we employed the vegetation index product (MOD13Q1) with 250 m spatial resolution and a compositing period of 16 days that is derived from Terra and Aqua satellite data (Huete et al. 2002; Solano et al. 2010). Data were downloaded for the period 2001–2011 from the Land Processes Distributed Active Archive Center (LP DAAC). Besides several ancillary layers such as quality, and angular information this product contains the Normalized Difference Vegetation Index (NDVI) and Enhanced Vegetation Index (EVI). It should be noted that Terra and Aqua composites are generated in phased production, i.e., the first composite of Terra uses the best observation between January 1st and 16th and Aqua between January 9th and 24th. Higher-level products such as MOD13 are offered in the form of a global grid where the Aral Sea region is entirely located in tile h22v04. Data were transformed to the Transverse Mercator projection centered at 60°E and WGS84 datum using the

MODIS Reprojection Tool (MRT). For visual interpretation cloud-free daily surface reflectance composites at 250 m spatial resolution were obtained for each year for dates between mid-August and mid-September (Vermote et al. 2002; MOD09GQ).

10.4 Methods

10.4.1 Desiccation Range Definition

In order to apply MODIS data time series for the above-mentioned topics firstly the yearly size of the Eastern and Western basins of the Aral Sea (both water bodies together composing the large Aral Sea) had to be determined. In order to extract the maximum dried area for each year, the minimum water extents of the water bodies for each year were derived. The results are "desiccation fringes", which represent the extent of the maximum desiccation process between the 2 years. Time series data of the last 11 years (2001–2011) were evaluated.

To derive the yearly minimum water extensions, so called "land-water masks" were calculated on a yearly basis using cloud-free MODIS surface reflectance data for the months of August and September, which usually reflect the smallest water body size at the end of the summer season after the highest evaporation impact. In addition, MODIS EVI products were used, because the water body can be better distinguished due to the lower index values in comparison to land and vegetation. Clear water bodies can usually be defined easily by this approach but the transition zones between water and land are more difficult as a result of the mixed signal between land and water. This is especially problematic for the Eastern basin due to the very shallow characteristic of this water body with very small water depths. This problem is less present in the Western basin due to a much steeper bathymetry and therefore EVI threshold values could be defined more easily for the land-water discrimination. Thus, a mixed approach was applied for the extraction of the water body of the Eastern basin, where the transition zones were defined visually and afterwards digitized manually complementing the masks for the deeper water bodies.

Secondly, after the derivation of the yearly water masks, four representative ground points were visually selected along the shorelines of the Western and Eastern basin within each annual desiccation fringe. Subsequently, these points were characterized using MODIS data products and associated time series plots. In order to provide a minimum 3 year observation period for the dried seabed, 2008 was selected as the final year.

10.4.2 Time Series Generation

A time series is a temporally ordered sequence of observations, commonly sampled at discrete intervals (Chatfield 2004). In remote sensing there are three broad categories of time series generation approaches: stacking, filtering and quality analysis with interpolation (Colditz et al. 2008a). The simplest approach stacks a number of co-registered satellite images. Since the Earth surface is often obscured by clouds and other atmospheric constituents or images have missing data, a number of images are used to form a composite using rules such as the maximum value (Holben 1986; Roy 2000) and the observation closest to nadir (Huete et al. 2002). In fact, since the early 1980s maximum value compositing has been used for time series generation of NOAA-AVHRR data. Techniques needed to be developed for cross-calibration between AVHRR satellites (Tucker et al. 2005). Filtering aims at eliminating remaining clouds and smoothing the time series. Common approaches include Harmonic Analysis for Time Series (HANTS, Roerink et al. 2000), an iterative approach that compares the original to a smoothed time series obtained by Fourier transformation and eliminates observations lower than a user-defined threshold, and Timesat (Jönsson and Eklundh 2004) that smoothes time series by Savitzky-Golay filtering, and Asymmetric Gaussian and Double logistic functions.

More recent sensor data and processing chains to derive value-added products, e.g. for MODIS, provide additional detailed information on the quality of each observation. The Quality Assessment Science Data Set (QA-SDS) indicates for each pixel the information about cloudiness, general processing state and other product-specific limitations (Roy et al. 2002). The Time Series Generator (TiSeG) analyzes the QA-SDS for all land products and calculates data availability indices according to user-defined quality specifications (Colditz et al. 2008a). The user may choose from a number of generic temporal interpolation methods or flag pixels with low data quality.

Time series of NDVI and EVI were generated combining TiSeG (version 1.3, Colditz et al. 2008a) and Timesat (version 3.1 beta, Jönsson and Eklundh 2004). Eight-day time series (2003–2011) were produced assuming alternation between 16-day composites of Terra and Aqua. Although alternation is not necessarily given, the potential error only relates to time translation but not amplitude and only the latter is of importance in this study. Two time series of different quality were generated: a simple stack of observations without data quality analysis and filtering (in the following denoted as layerstack, LS) and a filtered time series excluding pixels obscured by clouds or shadow with TiSeG and smoothed by a double logistic function in Timesat (in the following abbreviated with DL). Timesat was used with the following parameters: (1) median filter spike method with value 2, (2) forcing to one season, and (3) three iterations for upper envelope fitting with adaption strength 2. LS and DL time series for the years 2001 and 2002, when only Terra data were available, were produced apart from the combined Terra/Aqua time

series. The resulting 16-day composite time series was linearly interpolated to match the 8-day intervals to simplify further analysis.

10.5 Results and Discussion

10.5.1 Data Quality and Availability for Time Series Generation

Several studies have highlighted the use of MODIS quality information (Roy et al. 2002; Neteler 2005; Lunetta et al. 2006; Gao et al. 2008). Colditz et al. (2008a) compared various quality specifications and concluded that a strict quality (excluding many observations) may not be able to retain general time series characteristics due to an insufficient number of valid observations for temporal interpolation. A comparison between MODIS data versions (collections) concluded that using the current MODIS collection together with the pixel-level data quality information yields better and temporally more stable time series than the previous data collection (Colditz et al. 2008b). More automated time series generation techniques using MODIS quality information have been recently proposed for the vegetation index (VI, Colditz et al. 2011) and leaf area index (LAI, Gao et al. 2008; Yuan et al. 2011).

However, the applied quality specifications for the DL time series excluding only clouds and shadow are lenient in comparison to many other studies using MODIS vegetation index data. Colditz et al. (2008a) recommended that at least clouds, snow/ice and shadow should be excluded for time series over central Europe. Other studies are based on the usefulness index (UI, Lunetta et al. 2006; Colditz et al. 2006, 2011), a score that is derived from more detailed quality and angular information (Solano et al. 2010). Clouds (3) and shadow (2) combine a score of 5, equal to UI Intermediate or below (in case there are further quality issues), that is considered lenient (Colditz et al. 2008a) and only meaningful for areas with substantial quality issues such as tropical Africa (Colditz et al. 2006). Lunetta et al. (2006), for instance suggest using only observations of UI acceptable (maximum score 3) for the eastern United States. Although the study site is located in a dry region with mostly cloud-free observations throughout the summer months and comparatively little cloudiness during winter, there are substantial quality issues that are related to the spectral thresholds to define low data quality. Even though substantially improved, e.g. by a new backup algorithm for the EVI over high reflectance surfaces in the most recent data collection (Didan and Huete 2006; Colditz et al. 2008b; Solano et al. 2010), the algorithms still flag very flat specular surfaces, in particular if there is a salt crust that is often misinterpreted as snow and ice. Specular surfaces reflect radiation like a mirror if incoming and outgoing angles are similar. Water surfaces, on the other hand may be confused with shadow, if located close to a detected cloud.

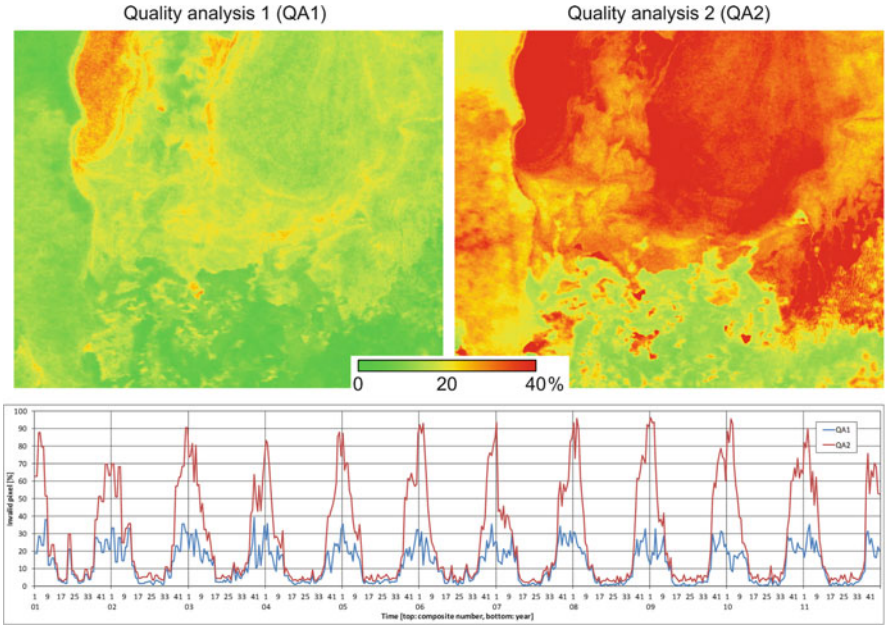

Fig. 10.1 Number of invalid pixels in space and time for two quality specifications (Note: QA1 excludes pixels that were identified as cloud and shadow. In addition QA2 excludes pixels flagged as snow/ice and with a usefulness index below fair (score 4))

Figure 10.1 depicts the proportion of invalid pixels spatially and temporally and compares two quality specifications: quality analysis QA1 excludes clouds and shadow and was used to generate the DL time series and QA2 excludes in addition a UI below fair (score 4) and pixels detected as snow and ice and thus is a typical setting for mid-latitudinal regions (Colditz et al. 2008a; Lunetta et al. 2006). Spatially, the comparison shows a much wider distribution of invalid pixels for QA2, in particular over water surfaces but also for desiccated areas of the Eastern basin and the developing Aralkum desert. The Amu Darya Delta region in the southern portion to the former coastline of the year 1960 shows relatively few invalid pixels also for the QA2 setting. The temporal plot illustrates that less data are available during the winter months (composite 37 to 11, corresponds to the end of October until the end of March). That coincides with the period of increased cloud cover. Setting QA2 more strictly shows higher proportions of invalid pixels during wintertime, also flagging existing ice on the Aral Sea as well as thin snow cover on the land. Still, the area proportion and length, especially for potential snow on the land, is clearly exaggerated.

An issue in time series generation is the length of the data gap to be interpolated (Colditz et al. 2008a, 2011). Although the period of invalid data between QA1 and QA2 seems similarly long, the temporal gap for QA1 is shorter for many pixels because short peaks up to 35 % invalid data soon drop below the 20 % threshold in

wintertime. This pattern is even better illustrated by the maximum gap statistic that measures the longest consecutive gap of data and therefore is a useful measure for the capability to interpolate data temporally. For time series filtered with QA1, 80 % of the data can be processed with a maximum gap of 6 composites (48 days). Similar measures for QA2 yield a maximum gap of 19 (152 days), that is the entire winter period as described above. The longest gaps are located in the inundating and desiccating areas of the Eastern and Western basin and the adjacent Aralkum desert and less in the permanent water bodies.

10.5.2 Regional Landscape Dynamics as a Consequence of Desiccation

Figure 10.2 illustrates the water body dynamics within the observed period 2001–2011. The colored lines represent the minimum extent of the water bodies during each year within the observation period. Clearly the general retreat of both water bodies can be observed as a consequence of the desiccation process. This trend is most obvious in the Eastern basin of the southern Aral Sea but is also observed along the eastern shoreline of the Western basin. Up to the year 2009 a general decline of the water surface can be documented. Seasonal water surface fluctuations can be significant and therefore the yearly documented desiccation refers to the maximum area between the minimum water extent of that year and the year before. The ranges of the desiccation fringe show a great variance, which is basically a function of micro-topography/bathymetry and available water inflow as potential evaporation does not change significantly over the years. Water availability is mainly determined by groundwater inflow (fairly constant), precipitation and surface runoff. The latter shows the largest intra-annual fluctuations, as principally affected by Amu Darya discharge, irrigation drainage water return flows from agricultural fields and water received by outflow from the North Aral Sea.

The dynamic of the desiccation process is generally high although less prominent in certain years such as the years 2002/2003 and 2003/2004. Nevertheless intra-annual changes in water body extent may be substantial as mentioned before and the yearly desiccation fringe may not be the result of a linear process but can also be affected by temporary flooding. The areas of the southern-most extension of the Eastern basin seem to show the highest landscape dynamics with respect to alternation of flooding and drying. The already dried seabed of the years prior to 2001 and 2002 were substantially flooded during the years 2003, 2004, 2005 and even 2010. The large flooding extensions of varying magnitude towards the south might also be the result of the changing topography and anthropogenic activities besides the yearly differences in hydrology. These flood events on the already dried seabed of different temporal length have consequences on the plant colonization process in these areas and on the growth dynamics of the sparse vegetation in general.

In the year 2009 for the first time a nearly complete temporary drying up of the Eastern basin water body was observed. On the other hand, in the following year of

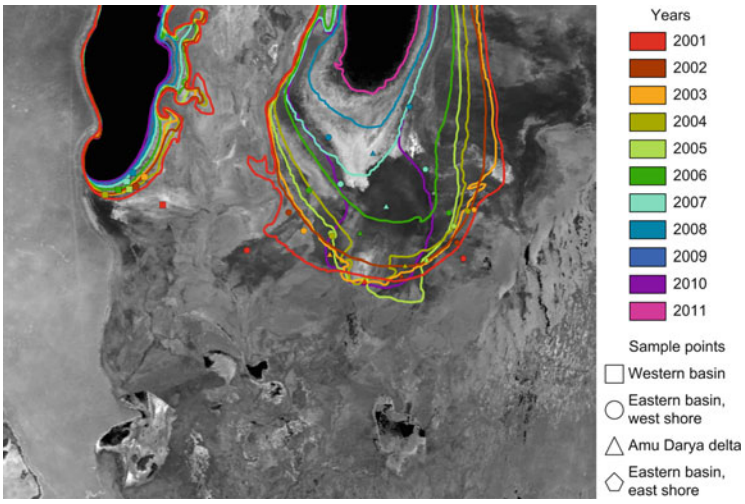

Fig. 10.2 Study area of southern Aral Sea with Western and Eastern basin (Note: The lines indicate the minimum water surface area derived from MODIS surface reflectance images between mid August and mid September for the respective years (*color*). The sample locations are indicated for each year (*color*) and site (*shape*). The image in the background shows the near infrared surface reflectance of September 15th 2011)

2010 the same water body of the Aral Sea showed a dramatic increase in surface size, resulting in a non-permanent flooding of large areas of seabed that dried up in earlier years. This year (2010) seems to show a rupture of the general desiccation trend. The Western basin in 2010, nevertheless, shows the smallest surface extent for the observation period, which was even less than the following year of 2011. It may be reasonable to conclude that this effect of the opposite desiccation dynamics of the two water bodies is caused by an exceptional discharge of the Amu Darya to the Eastern basin as a consequence of high precipitation during the winter month resulting in a strongly fluctuating hydrology (Breckle and Wucherer 2011).

To characterize these inter- and intra-annual changes concerning temporary flooding and potential vegetation dynamics, temporal profiles of the time series data of four annually selected observation points were analyzed. Figure 10.1 shows the distribution of these points within each desiccation fringe with the respective color of the shoreline of each individual year (minimum water extent).

10.5.3 Vegetation Index and Time Series for Landscape Dynamics

A vegetation index is a ratio between two or more spectral bands. In remote sensing the visual red and the near infrared bands are used to enhance vegetation patterns because of their high contrast with absorption due to plant pigments (chlorophyll a)

in the visual red band but reflection in the near infrared (Jensen 2007). A vegetation index such as the widely used Normalized Difference Vegetation Index (NDVI) is calculated by dividing the difference between the near infrared and the red band by the sum of both bands (Tucker 1979). The enhanced vegetation index also includes the blue band and soil correction factors to compensate for atmospheric disturbances and soil background (Huete et al. 2002). Normalization ensures that the index ranges between −1 and 1. In practice NDVI and the more recently developed EVI range between −0.2 and values close to 1. A negative vegetation index value can be observed over deep water with low sediment content and no aquatic vegetation. Bare soil shows slightly positive vegetation index values (0–0.1). Vegetation index values increase with increasing density of green, photosynthetically-active, healthy vegetation. Very high vegetation index values (0.8–1) may be measured over tropical regions, and in particular the NDVI begins to saturate.

Thus vegetation indices have a non-linear relationship to biophysical variables such as the Leaf Area Index or LAI (Myneni et al. 1997) and biomass (van der Meer et al. 2000). This saturation for high-biomass and very dense vegetation is compensated in the EVI that may show highest values of 0.7–0.8 but still with a non-linear relationship to biophysical variables. Besides, the EVI has been significantly improved in the most recent MODIS data collection. For surfaces such as snow and ice but also salt crusts, there is a high reflectance in the blue band that causes atmospheric over-correction (Didan and Huete 2006). Instead of using the Soil Adjusted Vegetation Index (SAVI) as in previous collections, MODIS collection 5 data employ a 2-band EVI (excluding the blue band), also known as EVI2 (Jiang et al. 2008). This was the main reason for presenting plots of the EVI instead of the NDVI in this study. However, plots of the NDVI show very similar ranges and only a few differences in the temporal course over the years.

The EVI DL and LS time series data plots were analyzed to illustrate the usefulness of MODIS time series to describe dynamic processes in the desiccated areas. The main interest was to investigate if the rather small vegetation dynamics on the newly dried seabed can be detected by the spectral sensitivity of the sensor. The assumption was that early plant succession on the newly desiccated areas might increase EVI values slightly over the years, which should be reflected in the time series. The natural process of plant colonization through halophytes and xerophytes is slow and our interest was to examine if an 11 year observation period would be sufficient to pick up any plant colonization trends over the entire period and if any intra-annual changes could be observed. The high temporal resolution of the MODIS sensor was expected to compensate to some degree for the lower spatial resolution in comparison to other imaging sensors. On the other hand, it could be hypothesized that the sparse vegetation would only result in small inter-annual changes in the EVI values and therefore in limited LS and DL time series value ranges. Additionally it could be supposed that the time series might eventually be noisy, as the landscape dynamics is rather high, especially along the Eastern basin due to the high inter annual fluctuations of the water extent between summer and winter months. As described above, eventually this results in temporary flooding of

the already dried seabed, which alters the EVI signal. It could be expected that the selected observation points along the shorelines within each yearly desiccation fringe could be affected by these inter annual changes, thus reflecting an associated yearly landscape dynamic.

10.5.4 General Description of Time Series and Trends

The graphs in Figs. 10.3 and 10.4 depict the EVI time series over 11 years of analysis (2001–2011). Each plot shows four samples (observation points) that dried in that year in comparison to the year before (for their spatial location see Fig. 10.1), except for the samples of 2001 that may have been dry for several years. For each year the samples were carefully selected at the southeastern shore of the Western basin (squares in Fig. 10.1, blue line in Figs. 10.3 and 10.4), the western shore of the Eastern basin (circles, red line), the Amu Darya Delta (triangles, green line), and the eastern shore of the Eastern basin (pentagons, orange line). The red bar at the bottom of each graph indicates the period of seabed drying for samples of that year, i.e. EVI, 2003 in Figs. 10.3 and 10.4 show the plots of samples that fell dry between 2002 and 2003 (minimum water extents in Fig. 10.2), thus the bar begins in 2003. Samples may inundate again in following years (not indicated by the red bars), as described before. Figure 10.3 presents the layerstack (LS) compared to Fig. 10.4 that shows the quality-filtered and smoothed double logistic time series (DL).

Before analyzing the plotted time series of Figs. 10.3 and 10.4, one should consider the very small dynamic range of the vegetation index (EVI) that, with a few exceptions, only varies between −0.2 and 0.1. Effectively, that describes the difference between water surfaces and barren land and thus highlights the landscape dynamics between advancing and retreating sea levels on an intra- and inter-annual temporal scale. Only one profile in 2001, sampled in the Amu Darya Delta, increased well above 0.2 (in DL up to 0.35 for the end of 2005 and with plateaus of 0.25 for the end of 2007 and 2008), that could be interpreted as a typical vegetation signal.

In comparison to the smooth curves of the DL time series the LS EVI plots show much noisier patterns with frequent positive and negative peaks with an EVI around 0. However, in relation to the potential range of the EVI (for MODIS the valid range is between −0.2 and 1) the variability is still small. On the contrary, some features that are visible in the LS disappear in the DL time series, e.g., some decreases of the EVI below 0 for the plot of EVI samples of 2006, 2007 and 2008 and in particular for the end of the year such as for samples of 2002 and the transition between 2003 and 2004. In the DL time series data were filtered for low quality, which mainly occurs during wintertime (see plot in Fig. 10.1). Applying low weights to those composites for a longer data gap paired with the strong smoothing characteristic of the double logistic function causes the DL plot to remain constant, although in reality the pixel should represent water as indicated by a slightly negative EVI. Potentially a more local smoothing function, e.g., a local box-car filter could have

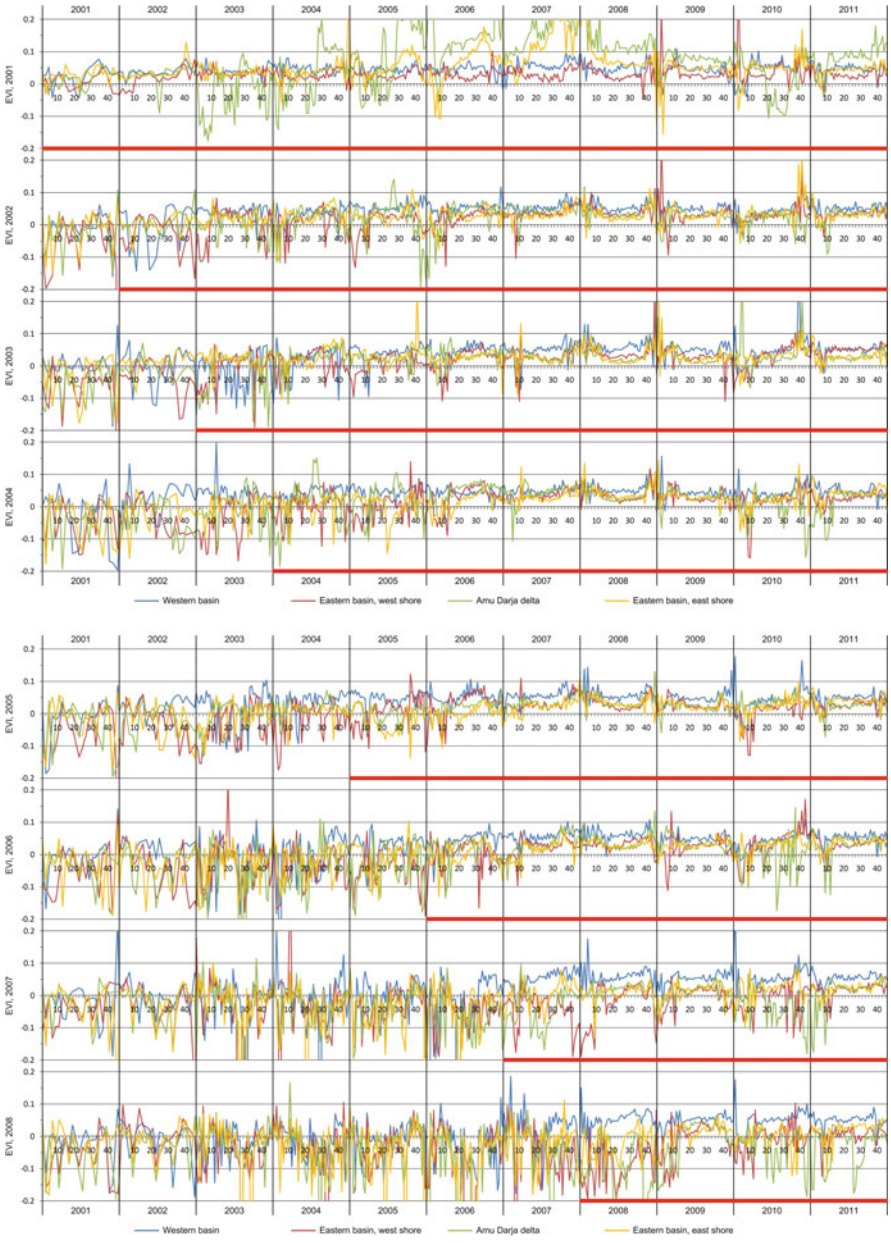

Fig. 10.3 Layerstack (*LS*) of EVI for samples collected in desiccation fringes of each year (see Fig. 10.2)

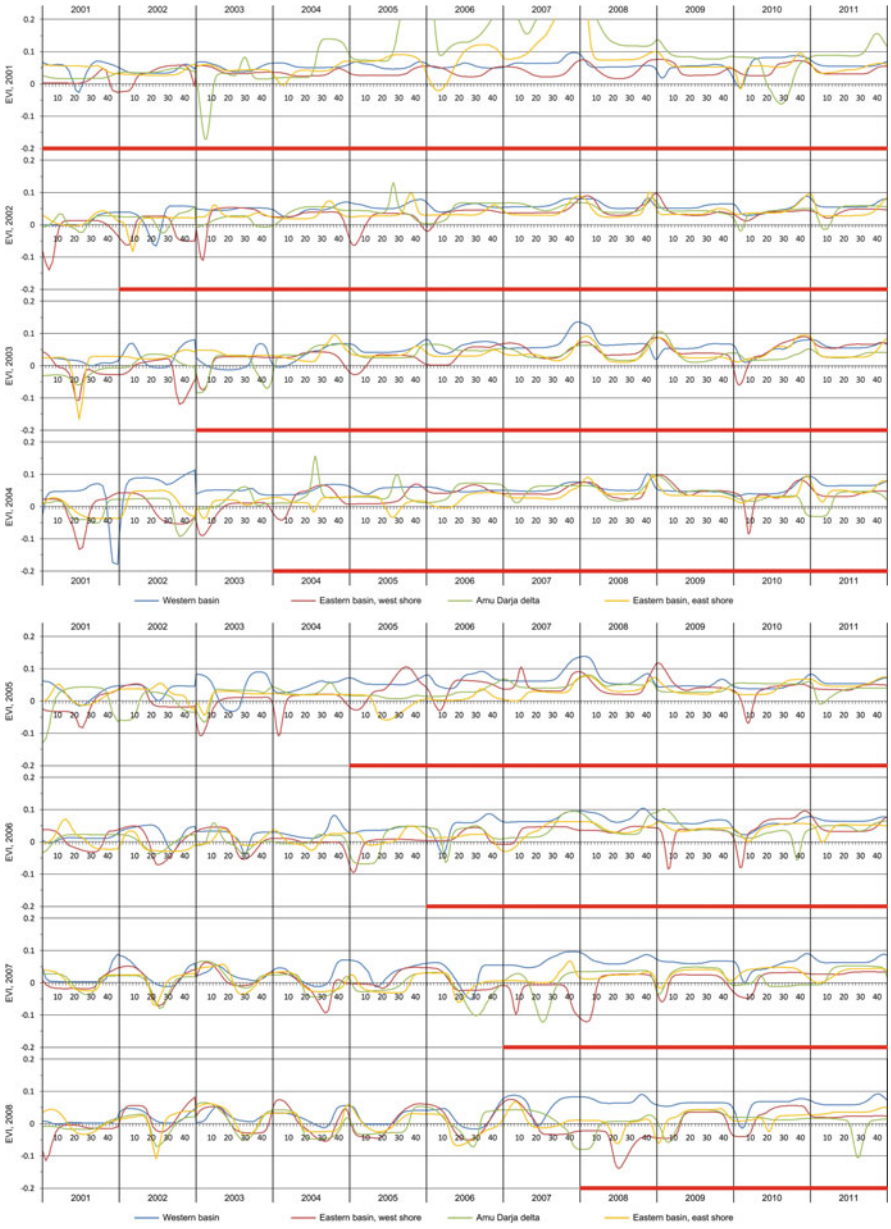

Fig. 10.4 Double logistic (*DL*) time series of EVI for samples collected in desiccation fringes of each year (see Fig. 10.2)

resolved this issue, but initial tests using a localized Savitzky-Golay filter of Timesat (Jönsson and Eklundh 2004) did not show satisfying results. In many other cases the DL function decreases for a short period, depending on available

vertexes for modeling during that period. Therefore the result of DL time series depends on the local temporal data availability by quality-filtered data and the generalization that was applied by a smoothing algorithm. Thus, the LS and DL time series have to be used together for the interpretation of landscape dynamics and desiccation patterns in the Aral Sea region.

A second feature is the displacement of EVI profiles between the end of 2002 and the beginning of 2003 for the DL time series. It should be noted that 2001 and 2002, when only Terra data were available, was processed apart from the period 2003 to 2011 with combined Terra/Aqua data. Although the year at the beginning and end of the time series were doubled to improve the stability at the temporal extremes of the time series (Jönsson and Eklundh 2004), also known as shouldering (Colditz et al. 2008a), fewer available data and a lack of overlap with the next actual year caused differences in curve fitting of the more global double logistic fitting function. However, the discontinuity in the time series is small and in most cases much less than 0.05.

A generalized analysis of plots over all years indicates a slightly positive slope. In fact, not a single slope showed a negative sign, albeit the increase is small. For instance the DL time series of the Western basin for the sample of 2007 shows a slope of 0.000121. The comparison of slopes between LS and DL time series shows almost constantly higher slopes for LS. This pattern is not surprising because many spikes were removed in the DL time series that generally were negative for the years 2001–2005 and became more positive for the period 2006–2011. Still, this pattern of declines for the earlier years and peaks for the later years during the winter period is notable in all time series. For instance the EVI samples of 2004 depict drops in the DL and a generally noisy pattern in LS time series for the period 2001–2004. The years 2005–2007 show less clear patterns in the DL but the LS also depicts a decreasing annual variability with a general tendency for increasing EVI values. For 2007 onwards most curves show more positive values during winter than for the rest of the year in DL and also in the LS time series (the exception is the west shore of the Eastern basin in 2010). The explanation of this pattern could be the permanent or frequent inundations of the sample points during the high water extents in the winter period, which causes the drop of EVI values (period 2001–2004). Although the sample became dry in 2004 in the minimum sea level mask, it may have inundated due to seasonal variations in 2005 and 2006 for shorter periods that were hardly detected by the DL time series but can still be noted by decreasing noise in the LS. With a longer distance from varying water levels the EVI shows a more steady soil signal (EVI between 0 and 0.1).

10.5.5 Particular Features in the Time Series

Despite the generally low dynamic range of the DL and LS time series several interesting features in the individual time plots can be observed. As already mentioned above there was an unusual flooding of the Eastern basin of the Aral

Sea in 2010 resulting in a large extension of the water body southward toward the Amu Darya Delta. This flooding mostly affected the central part of the Eastern basin and to a lesser degree the eastern and western shores and even reached the southern extent of the desiccation fringe of 2001. This effect can be seen in the EVI 2001 LS and DL time series plot within the portion for 2010. Clearly a steep decline of the EVI between the composites 17 and 41 (equivalent to the period between early May and mid November) of the year 2010 can be observed. In 2011 the EVI reaches rapidly positive values again throughout the year, which indicates the retreat of the exceptional flooding of the year 2010. The observation points of the years 2002, 2003, 2004 and 2005 appear to be less affected, some actually never reach negative EVI values, which seems to be consistent with their location as almost all points were only disturbed slightly during the maximum size increase of the water body or are located in the margins of the flooding zones. The observation points of the years of 2006, 2007 and 2008 nevertheless have been heavily affected by the flooding, which is also clearly reflected in the LS time series plot by a significant decline of the EVI values of these years in the summer month of 2010. Similar plot behavior can be observed at the observation points on the west shore of the Eastern basin, where the EVI drops to negative values in the years 2004, 2005, 2007 and 2008, but with a notable shift towards the beginning of the year. This may be explained by a larger flood extension towards the western part of the basin during the winter months.

The observation points collected at the Western basin show a different pattern in most plots. With the exception of samples from 2003, the samples hardly ever drop to values below 0 and show a steady curve with comparatively little variation also in the LS. The reason is the steeper gradient in topography in comparison to the Eastern basin. Once the samples became dry they are unlikely to inundate once again because of the steadily decreasing water level. The higher gradient of the shoreline makes it also less likely that seasonal water level changes can periodically or episodically flood samples taken at a higher level.

Looking at the intra-annual yearly dynamic of the DL time series, no significant peaks can be determined which could be related to the phenological activity of the sparse halophytic and xerophytic vegetation. Most likely is that early plant colonization during the observation period is not sufficiently dense to alter the EVI in a substantial way towards positive values. In other words, the MODIS signal in the desiccation fringes seems to be consistently dominated by the dry and sandy soils and salt crusts, which does not seem to change in a meaningful way even over the entire 11-year observation period. Even though plant colonization may progress over this time period, the MODIS signal appears not to pick up any associated changes concerning vegetation density or phenology.

Small changes towards the end of each year during the winter months may be observed in the EVI DL time series plots, but is less obvious in the observation points in the Amu Darya Delta. These small “peaks” at the end of the year seem to be surprising and cannot logically be related to a higher vegetation activity during these months.

10.6 Conclusions

MODIS time series data were analyzed for the Aral Sea and adjacent Amu Darya Delta for the years 2001–2011. The main interest was to evaluate the usefulness of MODIS surface reflectance data as well as 16-day EVI composites (linearly interpolated to 8-day intervals using phased Terra/Aqua production) for documenting the desiccation process in the Eastern and Western basin of the southern Aral Sea and potential vegetation dynamics. For each dried fringe four observation points were selected to describe the general desiccation trend as well as associated landscape and vegetation dynamics.

MODIS time series data have proven to be an excellent information source for analyzing the yearly desiccation process and for the discrimination of yearly newly dried seabed. As the water bodies of the southern Aral Sea show large inter- and intra-annual fluctuations, multi-temporal satellite data and products with a high temporal resolution are needed to quantify these dynamic processes. Through the combination of Terra/Aqua MODIS data, sufficient time series information can be provided to describe the water and landscape dynamics, although data has to be filtered and selected concerning quality. Very lenient quality parameters were chosen that only excluded clouds and shadows due to particular conditions on and around the Aral Sea with ice on the water, episodic snow cover during wintertime and salt flats that are spectrally similar to ice and snow and thus erroneously flagged by automated MODIS quality assessment algorithms. Otherwise, commonly used moderate quality specifications that also exclude snow and ice would have yielded unsatisfying results with respect to the potential to temporally interpolate data gaps.

The resulting EVI time series were subsequently analyzed using DL and LS plots. The DL time series provide smoother trends in comparison to the LS time series, which facilitates interpretation of the data series but may not provide the same detail as the LS time series, which on the other hand are significantly noisier. The general desiccation trend can be interpreted in both time series types. Overall, this landscape dynamic is reflected more clearly at the observation points in the desiccation fringes of the Western basin in comparison to the Eastern basin. This is due to the fact that inter- and intra-annual water body fluctuations are less frequent in the Western basin. More interestingly, particular events such as the prominent flooding of the year 2010 could be identified quite well in the time series plots including the impact of this flood on various observation points of the different years.

MODIS time series data nevertheless showed very limited use to describe vegetation dynamics on the newly desiccated areas over the 11-year observation period. Although a consistent and slightly positive trend of the EVI values was found, this tendency is not obvious enough to relate it to plant colonization activities. In addition no typical intra-annual plant phenology activity could be identified from the time series plots. This may be due to the fact that plant colonization is too slow and scarce within the observation period. Furthermore,

the high inter- and intra-annual dynamics of the water bodies, in particular of the Eastern basin of the Aral Sea, complicates plant colonization and growth, as pioneer species need to withstand repeated partial flooding by highly salinized water in addition to surviving the other harsh environmental conditions.

Finally, the MODIS sensor is not sufficiently sensitive to pick up small changes caused by the sparse vegetation as bare soil and sands dominate the signal. Longer observation periods may result in better outcomes as the vegetation density may increase with time. In order to compensate for this limitation, time series of satellite data with higher spatial resolution need to be applied to identify small regional changes and dynamics such as early plant colonization on the desiccation fringes.

Future studies with recently launched and upcoming satellite missions such as Rapideye, DMC, Sentinel-2 (ESA, launch 2014), Landsat-8 (launch 2013) will include the analysis of higher spatial resolution satellite data, to examine if partial plant colonization can be detected within the desiccation fringes of newly dried seabed. These systems will overcome limitations in spatial resolution of MODIS and will enhance the monitoring of landscape dynamics in general and plant succession dynamics in particular within the Amu Darya Delta and the Aral Sea region.

Acknowledgements We would like to thank F. Loew and C. Conrad, University of Wuerzburg, Department of Geography for the provision of in-situ data for the year 2008 as well as a satellite-based classification for the Amu Darya Delta.

References

Breckle SW, Wucherer W (2011) Has the Aral Sea a future. In: Lozán JL, Grassl H, Hupfer P, Menzel L et al (Hrsg) Warnsignal Klima: Genug Wasser fuer alle? Wissenschaftliche Auswertungen in Kooperation mit Geo, 3.Auflage (2011), pp 131–135 (in German)

Breckle SW, Wucherer W, Dimeyeva LA, Ogar NP (eds) (2012) Aralkum – a man-made desert. The desiccated floor of the Aral Sea (Central Asia), vol 218, Ecological studies. Springer, Berlin/Heidelberg. doi:10.1007/978-3-642-21117-16

Chatfield C (2004) The analysis of time series: an introduction. Chapman & Hall, London

Colditz RR, Conrad C, Wehrmann T, Schmidt M et al (2006) Generation and assessment of MODIS time series using quality information. In IEEE international conference on geoscience and remote sensing 2006, IGARSS 2006, July 31st–August 4th 2006, Denver, pp 779–782

Colditz RR, Conrad C, Wehrmann T, Schmidt M et al (2008a) TiSeG – a flexible software tool for time series generation of MODIS data utilizing the quality assessment science data set. IEEE Trans Geosci Remote Sens 46(10):3296–3308

Colditz RR, Conrad C, Wehrmann T, Schmidt M et al (2008b) Analysis of the quality of collection 4 and 5 vegetation index time series from MODIS. In: Stein A, Shi W, Bijker W (eds) Quality aspects in spatial data mining. CRC Press, Boca Raton, pp 161–174 (Also published in ISPRS Spatial Data Quality Symposium, June 13th–15th 2007, Enschede, The Netherlands)

Colditz RR, Conrad C, Dech S (2011) Stepwise automated generation of time series using ranked data quality indicators. IEEE J Sel Top Appl Earth Observ Remote Sens 4(2):272–280

Conrad C, Dech SW, Hafeez M, Lamers J, Martius C, Strunz G (2007) Mapping and assessing water use in a Central Asian irrigation system by utilizing MODIS remote sensing products.

Irrig Drain Syst 21:197–218. doi:10.1007/s10795-007-9029-z (Dordrecht: Springer Science + Business Media B.V)
Didan K, Huete AR (2006) MODIS vegetation index product series collection 5 change summary. The University of Arizona, Tucson, June 29th
Gao F, Morisette JT, Wolfe RE, Ederer G et al (2008) An algorithm to produce temporally and spatially continuous MODIS-LAI time series. IEEE Geosci Remote Sens Lett 5(1):60–64
Ginzburg AI, Kostianoy AG, Sheremet NA, Kravtsova VI (2010). Satellite monitoring of the Aral Sea region. In: The Aral Sea Envioronment. Series: The handbook of Environmental Chemistry, Series ISSN 1867-979X, DOI 10.1007/698_2009_15, ISBN: 978-3-540-88276-3, pp. 147–179
Glazovskiy NF (1990) The Aral crisis: causative factors and means of solution. Nauka, Moscow (In Russian)
Hansen MC, DeFries RS, Townshend JRG, Sohlberg RA (2000) Global land cover classification at 1 km spatial resolution using a classification tree approach. Int J Remote Sens 21 (6–7):1331–1364
Holben BN (1986) Characterization of maximum value composites from temporal AVHRR data. Int J Remote Sens 7(11):1417–1434
Huete AR, Didan K, Miura T, Rodriguez EP et al (2002) Overview of the radiometric and biophysical performance of the MODIS vegetation indices. Remote Sens Environ 83 (1–2):195–213
Jensen RR (2007) Remote sensing of the environment. Prentice Hall, Upper Saddle River
Jiang Z, Huete AR, Didan K, Miura T (2008) Development of a two-band enhanced vegetation index without a blue band. Remote Sens Environ 112:3833–3845
Jönsson P, Eklundh L (2004) TIMESAT – a program for analyzing time-series of satellite sensor data. Comput Geosci 30:833–845
Justice CO, Townshend JRG, Vermote EF, Masuoka E et al (2002) An overview of MODIS land data processing and product status. Remote Sens Environ 83(1–2):3–15
Kidwell KB (1991) NOAA polar orbiter data users guide. National Oceanic and Atmospheric Administration, National Environmental Satellite Data and Information Service, Washington, DC
Loew F, Navratil P, Bubenzer O et al (2012) Landscape dynamics in the Southern Aralkum. Using MODIS time series for land cover change analysis. In: Breckle SW (ed) Aralkum a man made desert: the desiccated floor of the Aral Sea (Central Asia), Ecological studies 218. Springer, Berlin/Heidelberg. doi:10.1007/978-3-642-21117-16
Lunetta RS, Knight JF, Ediriwickrema J, Lyon J et al (2006) Land-cover change detection using multi-temporal MODIS NDVI data. Remote Sens Environ 105(2):142–154
Micklin P (2004) The Aral Sea crisis. In: Nihoul CJ, Zavialov P, Micklin P (eds) Dying and dead seas: climatic vs. anthropic causes, NATO science series IV: Earth and environmental sciences, 36th edn. Kluwer, Boston, pp 99–125
Micklin P (2007) The Aral Sea disaster. Annu Rev Earth Planet Sci 35:47–72, Palo Alto: Annual Reviews
Myneni RB, Nemani RR, Running SW (1997) Estimation of global leaf area index and absorbed par using radiative transfer models. IEEE Trans Geosci Remote Sens 35(6):1380–1393
Neteler M (2005) Time series processing of MODIS satellite data for landscape epidemiological applications. Int J Geoinf 1(1):133–138
Novikova N (1996a) The Tugai of the Aral Sea region is dying: can it be restored? Russ Conserv News 6:22–23
Novikova N (1996b) Current changes in the vegetation of the Amu Darya Delta. In: Micklin P, Williams D (eds) The Aral Sea Basin. In Proceedings of the NATO advanced research workshop, Tashkent, Uzbekistan 2–5 May, NATO ASI Series, 2. Environment, vol 12. Springer, New York, pp 69–78
Novikova N (1997) Principles of preserving the botanical diversity of the deltaic plains of the Turan. Dissertation for the degree of Doctor of Geographical Sciences. Moscow (in Russian)

Ptichnikov A (ed) (2002) Bulletin no 3, NATO science for peace project 974101: sustainable development of ecology, land and water use through implementation of a GIS and remote sensing centre in Karakalpakstan (in Russian and English)

Ressl RA (1996) Monitoring of recent area and volume changes of the Aral Sea and development of an optimized land and water use model for the Amu Darya Delta. In: Micklin P, Williams D (eds) The Aral Sea Basin. In Proceedings of the NATO advanced research workshop, Tashkent, Uzbekistan 2–5 May, NATO ASI Series, 2. Environment, vol 12. Springer, New York, pp 149–160

Ressl RA, Dech SW, Ptichnikov A, Novikova NM, Micklin P (1998) Aufbau eines fernerkundungsbasierten geographischen informationssystems zur optimierung der landnutzung im Amu Darya delta. (Development of a remote sensing based geographical information system for optimizing landuse in the Amu Darya delta). GIS Geo Inf Syst 11:25–33 (in German)

Roerink GJ, Menenti M, Verhoef W (2000) Reconstructing cloud free NDVI composites using fourier analysis of time series. Int J Remote Sens 21(9):1911–1917

Roy DP (2000) Investigation of the maximum Normalized Difference Vegetation Index (NDVI) and the maximum surface temperature (Ts) AVHRR compositing procedure for the extraction of NDVI and Ts over forests. Int J Remote Sens 18(11):2383–2401

Roy DP, Borak JS, Devadiga S, Wolfe RE et al (2002) The MODIS land product quality assessment approach. Remote Sens Environ 83(1–2):62–76

Solano R, Didan K, Jacobson A, Huete A (2010) MODIS vegetation index user's guide (MOD13 series). Version 2.0, (Collection 5)

Thenkabail PS, Schull M, Turral H (2005) Ganges and indus river basin land use/land cover (LULC) and irrigated area mapping using continuous streams of MODIS data. Remote Sens Environ 95:317–341

Tucker CJ (1979) Red and photographic infrared linear combinations for monitoring vegetation. Remote Sens Environ 8(2):127–150

Tucker CJ, Pinzon JE, Brown ME, Slayback DA et al (2005) An extended AVHRR 8-km NDVI dataset compatible with MODIS and SPOT vegetation NDVI data. Int J Remote Sens 26 (20):4485–4498

Van der Meer F, Bakker W, Scholte K, Skidmore A et al (2000) Vegetation indices, above ground biomass estimates and the red edge from MERIS. Int Arch Photogramm Remote Sens 33 (Part B7):1580–1586

Vermote EF, el Saleous NZ, Justice CO (2002) Atmospheric correction of MODIS data in the visible to middle infrared: first results. Remote Sens Environ 83(1–2):97–111

Yuan H, Dai Y, Xiao Z, Ji D et al (2011) Reprocessing the MODIS leaf area index products for land surface and climate modeling. Remote Sens Environ 115:1171–1187